ELSEVIER

Journal of Organometallic Chemistry 485 (1995) 191–199

Journal of Organometallic Chemistry

The heteronuclear cluster chemistry of the Group IB metals Part XVII ☆. Synthesis and X-ray crystal structure of the hexanuclear mixed-metal cluster $[Ag_2Ru_4(\mu_3\text{-}H)_2(CO)_{12}\{P(C_6H_4Me\text{-}2)_3\}_2]$. An investigation of the steric properties of the $P(C_6H_4Me\text{-}2)_3$ ligand

Paul J. McCarthy [a,1], Ian D. Salter [a,*], Trushar Adatia [b]

[a] *Department of Chemistry, University of Exeter, Exeter EX4 4QD, UK*
[b] *School of Chemistry, University of North London, London N7 8DB, UK*

Received 14 April 1994

Abstract

Treatment of a dichloromethane solution of the salt $[N(PPh_3)_2]_2[Ru_4(\mu\text{-}H)_2(CO)_{12}]$ with two equivalents of the complex $[Ag(NCMe)_4]PF_6$ at −30°C, followed by the addition of two equivalents of the very bulky phosphine ligand $P(C_6H_4Me\text{-}2)_3$ (cone angle 194°) affords the mixed-metal cluster $[Ag_2Ru_4(\mu_3\text{-}H)_2(CO)_{12}\{P(C_6H_4Me\text{-}2)_3\}_2]$ (**I**) in ca. 70% yield. A single-crystal X-ray diffraction study has revealed that **I** has a capped trigonal bipyramidal metal framework structure, with the two silver atoms in close contact [Ag–Ag 2.876(2) Å]. This skeletal geometry is very surprising in view of a previous observation that P^tBu_3 (cone angle 182°), which is supposedly a less sterically demanding phosphine ligand than $P(C_6H_4Me\text{-}2)_3$, is sufficiently bulky to prevent the two $Ag(P^tBu_3)$ units being adjacent in the metal core of the closely related cluster $[Ag_2Ru_4(\mu_3\text{-}H)_2(CO)_{12}(P^tBu_3)_2]$. In the solid-state structure of **I**, it appears that two of the three $C_6H_4Me\text{-}2$ rings in each of the two $P(C_6H_4Me\text{-}2)_3$ ligands can adopt relative orientations which allow the phosphine to behave as a less sterically demanding ligand than its large cone angle might otherwise suggest. Remarkably, the formal replacement of the two PPh_3 ligands attached to the silver atoms in the capped trigonal bipyramidal metal framework of the closely related cluster $[Ag_2Ru_4(\mu_3\text{-}H)_2(CO)_{12}(PPh_3)_2]$ by two $P(C_6H_4Me\text{-}2)_3$ groups in **I** causes very little change in most of the metal–metal distances, despite the fact that the cone angle of PPh_3 (145°) is 49° smaller than that of $P(C_6H_4Me\text{-}2)_3$. In solution, compound **I** undergoes two types of dynamic behaviour at ambient temperatures. One process involves an intramolecular rearrangement of the metal core, which exchanges the two silver atoms between the two inequivalent sites, and the other process is an intermolecular exchange of $P(C_6H_4Me\text{-}2)_3$ ligands between clusters.

Keywords: Group 11; Silver; Ruthenium; Phosphine ligands; Cone angles; Crystal structure

1. Introduction

One of the novel features of many Group IB (Group 11) metal heteronuclear cluster compounds is the degree of flexibility exhibited by their metal frameworks, both in the solid state and in solution, when the nature of the phosphine ligand(s) attached to the coinage metals is varied [2–4]. Some of us [5–9] have recently demonstrated that an increase in the cone angle [10] of the monodentate phosphine ligands attached to the coinage metals in the clusters $[M_2Ru_4H_2(CO)_{12}(PR_3)_2]$ (M = Cu, Ag, or Au; R = alkyl or aryl) can alter the metal core geometry adopted by these species in the solid state. Our results (Table 1) show that this class of cluster compound can exhibit one of two distinct metal framework structures. In structure A (Fig. 1), the two Group IB metals are in close contact, whereas in structure B no bonding interaction is observed between the coinage metals (Fig. 1). The capped trigonal bipyramidal structure A is preferred for clusters containing P^iPr_3 (cone angle 160° [10]) [6], PPh_3 (cone

☆ For Part XVI, see ref. 1.

* Corresponding author.

[1] Present address: Exchem Industries Ltd., Great Oakley Works, Great Oakley, Harwich, Essex, CO12 5JW, UK.

SSDI 0022-328X(94)24774-D

Table 1
The metal framework structures adopted by the mixed-metal clusters $[M_2Ru_4(\mu_3\text{-}H)_2(CO)_{12}L_2]$

M	L	Cone angle of L [a] (°)	Metal framework structure [b]	Ref.
Cu	PMe_2Ph, PMe_3, or PEt_3	≤ 122	A	[8]
Cu	$P(OR)_3$ (R = Ph, Me, or Et)	≤ 128	A	[8]
Cu or Ag	PMe_2Ph	136	A	[8,9]
Cu, Ag, or Au	PPh_3	145	A	[7]
Cu	P^iPr_3	160	A [c]	[6]
Ag or Au	P^iPr_3	160	A	[6]
Cu	$P(CH_2Ph)_3$	165	B	[5]
Ag	$P(CH_2Ph)_3$	165	A	[5]
Cu	PCy_3	170	B	[6]
Ag or Au	PCy_3	170	A	[6]
Ag or Au [d]	P^tBu_3	182	B	[6]

[a] Ref. [10]. [b] See Fig. 1 for diagrams of the two skeletal geometries. [c] Although $[Cu_2Ru_4(\mu_3\text{-}H)_2(CO)_{12}(P^iPr_3)_2]$ adopts structure A in the solid state, the P^iPr_3 ligand is bulky enough for a second skeletal isomer, which is thought to have two face-capping $Cu(P^iPr_3)$ fragments with no Cu–Cu close contact, to also be present in solution [6]. [d] Attempts to prepare the copper-containing analogue resulted in the isolation of the pentanuclear species $[CuRu_4(\mu_3\text{-}H)_3(CO)_{12}(P^tBu_3)]$ instead of the expected hexanuclear cluster $[Cu_2Ru_4(\mu_3\text{-}H)_2(CO)_{12}(P^tBu_3)_2]$ [6].

angle 145° [10]) [7] and smaller phosphine and phosphite ligands [8,9]. However, the $P(CH_2Ph)_3$ (cone angle 165° [10]) [5] and PCy_3 (cone angle 170° [10]) [6] ligands are too bulky to allow two $Cu(PR_3)$ (R = CH_2Ph or Cy) units to be adjacent in the metal frameworks of $[Cu_2Ru_4(\mu_3\text{-}H)_2(CO)_{12}(PR_3)_2]$ and these clusters are forced to adopt the sterically less demanding edge-bridged trigonal bipyramidal structure B. The greater size of the silver and gold atoms relative to copper means that two adjacent $M(PR_3)$ (M = Ag, R = CH_2Ph or Cy; M = Au, R = Cy) units can be accommodated in the metal skeletons of $[M_2Ru_4(\mu_3\text{-}H)_2(CO)_{12}(PR_3)_2]$ [5,6]. The even larger phosphine ligand P^tBu_3 (cone angle 182° [10]) is required to force the silver- and gold-containing cluster compounds to alter their skeletal geometries to structure B [6]. In view of these results, we thought it of interest to prepare Group IB metal heteronuclear clusters containing the very bulky phosphine ligand $P(C_6H_4Me\text{-}2)_3$ (cone angle 194° [10]).

2. Results and discussion

Treatment of a dichloromethane solution of the salt $[N(PPh_3)_2]_2[Ru_4(\mu\text{-}H)_2(CO)_{12}]$ with two equivalents of

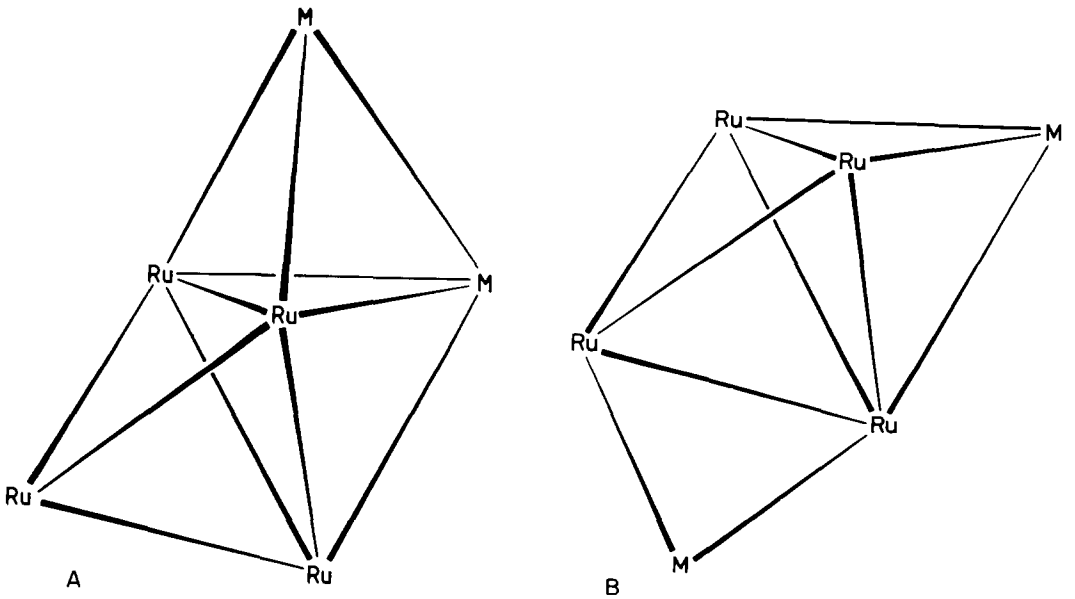

Fig. 1. The capped trigonal bipyramidal (structure A) and the sterically less demanding edge-bridged trigonal bipyramidal (structure B) skeletal geometries adopted by the clusters $[M_2Ru_4(\mu_3\text{-}H)_2(CO)_{12}L_2]$ [M = Cu, Ag, or Au; L = a variety of monodentate phosphine and phosphite ligands (see Table 1)].

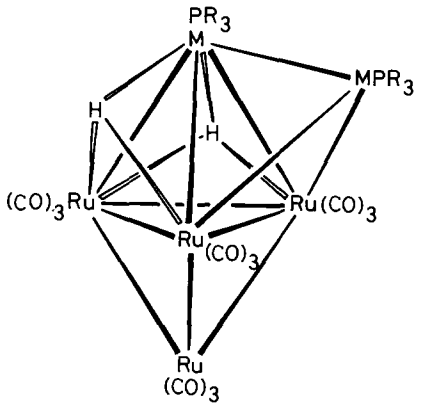

	M	R
I	Ag	C_6H_4Me-2
II	Ag	Ph
III	Cu	Ph

the complex $[Ag(NCMe)_4]PF_6$ at −30°C, followed by the addition of two equivalents of $P(C_6H_4Me\text{-}2)_3$ affords the red cluster compound $[Ag_2Ru_4(\mu_3\text{-}H)_2(CO)_{12}\{P(C_6H_4Me\text{-}2)_3\}_2]$ (**I**) in ca. 70% yield. Surprisingly, the infrared spectrum of **I** closely resembles that reported [7] for the analogous PPh_3-containing cluster $[Ag_2Ru_4(\mu_3\text{-}H)_2(CO)_{12}(PPh_3)_2]$ (**II**), but it is significantly different from that observed for $[Ag_2Ru_4(\mu_3\text{-}H)_2(CO)_{12}(P^tBu_3)_2]$ [6]. Thus, the infrared spectroscopic data imply that **I** adopts the capped trigonal bipyramidal metal core structure A (Fig. 1) rather than the sterically less-demanding edge-bridged trigonal bipyramidal skeletal geometry B, despite the considerable size of the $P(C_6H_4Me\text{-}2)_3$ ligand. Variable-temperature ^1H and $^{31}P\text{-}\{^1H\}$ NMR spectroscopic studies on **I** provided little useful structural information about the cluster compound because of its poor solubility in all common organic solvents which severely hindered the recording of good spectra at low temperatures, and because of the broadening of the spectra due to dynamic behaviour in solution (vide infra). Therefore, it was of interest to perform a single-crystal X-ray diffraction study on **I** and to have the opportunity to compare the structural data of **I** with those previously determined [7] for the analogous cluster **II**. Discussion of the variable-temperature ^1H and $^{31}P\text{-}\{^1H\}$ NMR spectroscopic data for **I** is best deferred until the X-ray diffraction results have been presented.

The molecular structure of **I** is displayed in Fig. 2 and selected interatomic distances and angles are listed in Table 2. The metal framework of **I** consists of a Ru_4 tetrahedron, with one Ru_3 [Ru(1)Ru(3)Ru(4)] face capped by a silver atom [Ag(2)] and one $AgRu_2$ face [Ag(2)Ru(3)Ru(4)] of the $AgRu_3$ tetrahedron so formed capped by the second silver atom [Ag(1)], so that the two silver atoms are in close contact. Therefore, the X-ray diffraction study confirms that **I** adopts metal core structure A (Fig. 1), as suggested by the infrared spectroscopic data. One $P(C_6H_4Me\text{-}2)_3$ ligand is attached to each of the two silver atoms, as expected, and each ruthenium atom is ligated by three essentially linear carbonyl groups. The two hydrido ligands cap two adjacent $AgRu_2$ faces [Ag(2)Ru(1)Ru(3) and Ag(2)Ru(1)Ru(4)]. The overall structure of **I** is very similar to that established for its PPh_3-containing analogue **II** [7].

Fig. 3 compares the metal–metal separations within the skeletal frameworks of **I** and **II**. The range of Ru–Ru distances in **I** [2.774(2)–2.978(2) Å] is similar to that in **II** [2.785(1)–2.979(1) Å]. As expected [11,12], none of the equivalent Ru–Ru separations are changed greatly and five out of the six differ by only ca. 0.011 Å or less (Fig. 3). In fact, the mean Ru–Ru bond length in **I** [2.879(2) Å] is only 0.003 Å shorter than that in **II** [2.882(1) Å]. The range of Ag–Ru distances found for the hexanuclear cluster **I** [2.862(2) – 3.045(2) Å] is slightly higher than that observed for the PPh_3-containing analogue **II** [2.842(1)–2.980(1) Å], but three out of the five separations exhibit differences of ca. 0.021 Å or less (Fig. 3). However, the mean Ag–Ru separation of 2.925(2) Å in **I** is 0.037 Å longer than the mean Ag–Ru distance calculated for cluster **II**. In both of the clusters **I** and **II**, all of the three Ag–Ru distances to the Ag atom in the equatorial plane of the trigonal bipyramidal Ag_2Ru_3 unit [Ag(2)–Ru(1), Ag(2)–Ru(3) and Ag(2)–Ru(4)] appear to be markedly longer than those to the Ag atom occupying the axial site (Fig. 3). However, two of the three Ag–Ru bonds involving the equatorial Ag atom in **I** are substantially longer than the equivalent bonds in **II**, by ca. 0.065 Å [Ag(2)–Ru(1)] and 0.108 Å [Ag(2)–Ru(4)]. In contrast, the Ag–Ag distance is only increased by ca. 0.019 Å when the two

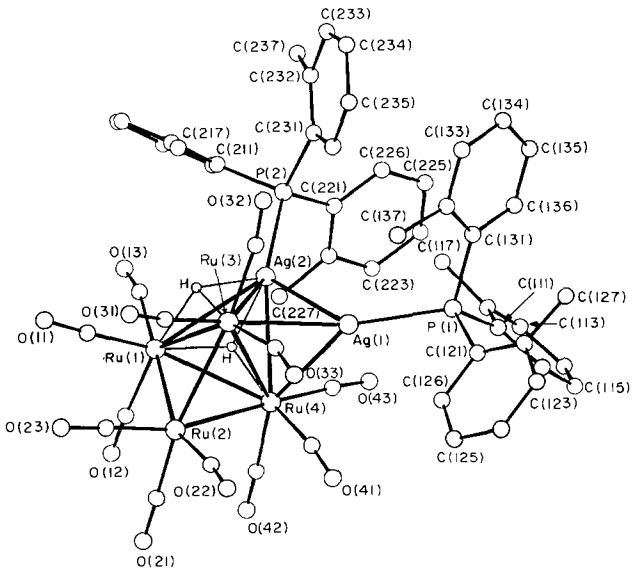

Fig. 2. Molecular structure of $[Ag_2Ru_4(\mu_3\text{-}H)_2(CO)_{12}\{P(C_6H_4Me\text{-}2)_3\}_2]$ (**I**), showing the crystallographic numbering. The carbon atom of each carbonyl ligand has the same number as the oxygen atom.

PPh_3 groups in **II** are formally replaced by $P(C_6H_4$-Me-2$)_3$ ligands in **I**.

Remarkably, Fig. 3 shows that an increase of 49° in the magnitude of the cone angle of the attached phosphine ligands has very little effect on most of the metal–metal separations in the metal skeletons of **I** and **II**. In marked contrast to this observation, the formal replacement of the two PPh_3 ligands in the structurally related cluster $[Cu_2Ru_4(\mu_3\text{-}H)_2(CO)_{12}$-$(PPh_3)_2]$ (**III**) by P^iPr_3, which corresponds to an increase in cone angle of only 15°, is known [7,13] to result in elongation of the Cu–Cu bond by ca. 0.311 Å in the solid state. In addition, the same formal change of ligands causes the lengths of two of the five Cu–Ru bonds to increase by more than 0.2 Å and one by ca. 0.1 Å [7,13]. The generally small differences observed between the equivalent metal–metal distances in **I** and **II** are also very surprising in view of the well established 'softness' of the bonding between Group IB metals themselves and between coinage metals and other transition metals [2–4]. For example, significant differences have been observed [11] between some of the equivalent metal–metal separations in the two independent molecules which occur in the asymmetric unit of $[Cu_2Ru_4(\mu_3\text{-}H)_2\{\mu\text{-}Ph_2P(CH_2)_2PPh_2\}(CO)_{12}]$, and crystal packing forces are known [14] to cause differences of up to 0.091 Å between the equivalent metal–metal distances in the metal frameworks of the two crystalline modifications of $[Au_2Ru_4(\mu_3\text{-}H)(\mu\text{-}H)$-$(\mu\text{-}Ph_2PCH_2PPh_2)(CO)_{12}]$.

The fact that the $P(C_6H_4Me\text{-}2)_3$ groups in **I** appear to act as smaller phosphine ligands than the cone angle of 194° [10] would suggest may be attributed to the ability of some of the C_6H_4Me-2 rings on the two adjacent phosphine molecules to align in a manner which decreases the expected large steric repulsion between two ligands. Fig. 4 shows the views down the P(1)–Ag(1) and P(2)–Ag(2) bonds in **I** to illustrate the relative alignments of the six C_6H_4Me-2 rings. It can be seen that the C_6H_4Me-2 rings on the two phosphine ligands are able to adopt relative positions which avoid any really serious repulsive interactions between the *ortho* methyl groups. Thus, although the *ortho* methyl groups cause the $P(C_6H_4Me\text{-}2)_3$ ligand to have a much larger cone angle than that of PPh_3, the ability of the C_6H_4Me-2 rings in two adjacent phosphine ligands to position themselves in such a way as to minimize repulsive interactions between those methyl groups means that $P(C_6H_4Me\text{-}2)_3$ can act as a much less bulky ligand than its cone angle might otherwise suggest.

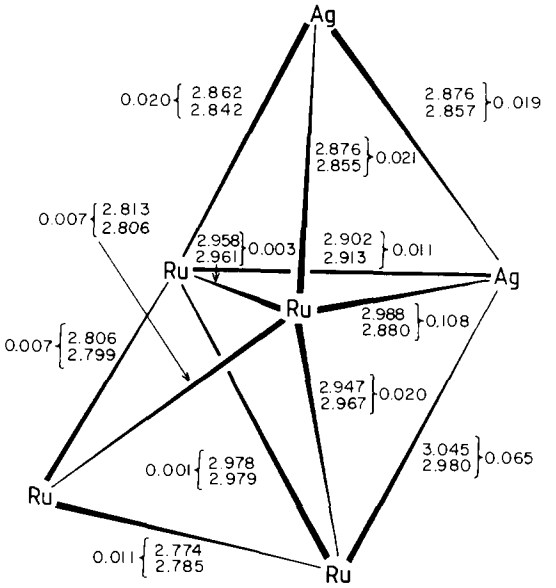

Fig. 3. A comparison of the metal-metal separations in the metal frameworks of $[Ag_2Ru_4(\mu_3\text{-}H)_2(CO)_{12}(PR_3)_2]$ [R = C_6H_4Me-2 (**I**) or Ph (**II**)]. Distances are given first for **I** and then for **II** [7].

Table 2
Selected bond lengths (Å) and angles (°) for $[Ag_2Ru_4(\mu_3\text{-}H)_2(CO)_{12}\{P(C_6H_4Me\text{-}2)_3\}_2]\cdot CH_2Cl_2$, with estimated standard deviations in parentheses

(a) Bond lengths			
Ru(1)–Ru(2)	2.774(2)	Ru(1)–Ru(3)	2.978(2)
Ru(1)–Ru(4)	2.947(2)	Ru(1)–Ag(2)	3.045(2)
Ru(2)–Ru(3)	2.806(2)	Ru(2)–Ru(4)	2.813(2)
Ru(3)–Ru(4)	2.958(2)	Ru(3)–Ag(1)	2.862(2)
Ru(3)–Ag(2)	2.902(2)	Ru(4)–Ag(1)	2.876(2)
Ag(1)–Ag(2)	2.876(2)	Ru(4)–Ag(2)	2.988(2)
Ag(2)–P(2)	2.466(5)	Ag(1)–P(1)	2.494(5)
Range of Ru–C(CO)		1.755(8)–1.996(7)	
Range of C–O(CO)		1.108(8)–1.210(11)	
Range of P–C(C_6H_4Me–2)		1.784(8)–1.829(8)	
(b) Bond angles			
Ru(3)–Ru(1)–Ru(2)	58.3(1)	Ru(4)–Ru(1)–Ru(2)	58.8(1)
Ru(4)–Ru(1)–Ru(3)	59.9(1)	Ag(2)–Ru(1)–Ru(2)	106.1(1)
Ag(2)–Ru(1)–Ru(3)	57.6(1)	Ag(2)–Ru(1)–Ru(4)	59.8(1)
Ru(3)–Ru(2)–Ru(1)	64.5(1)	Ru(4)–Ru(2)–Ru(1)	63.7(1)
Ru(4)–Ru(2)–Ru(3)	63.5(1)	Ru(2)–Ru(3)–Ru(1)	57.2(1)
Ru(4)–Ru(3)–Ru(1)	59.5(1)	Ru(4)–Ru(3)–Ru(2)	58.3(1)
Ag(1)–Ru(3)–Ru(1)	109.4(1)	Ag(1)–Ru(3)–Ru(2)	110.9(1)
Ag(1)–Ru(3)–Ru(4)	59.2(1)	Ag(2)–Ru(3)–Ru(1)	62.4(1)
Ag(2)–Ru(3)–Ru(2)	109.2(1)	Ag(2)–Ru(3)–Ru(4)	61.3(1)
Ag(2)–Ru(3)–Ag(1)	59.8(1)	Ru(2)–Ru(4)–Ru(1)	57.5(1)
Ru(3)–Ru(4)–Ru(1)	60.6(1)	Ru(3)–Ru(4)–Ru(2)	58.1(1)
Ag(1)–Ru(4)–Ru(1)	109.9(1)	Ag(1)–Ru(4)–Ru(2)	110.3(1)
Ag(1)–Ru(4)–Ru(3)	58.7(1)	Ag(2)–Ru(4)–Ru(1)	61.7(1)
Ag(2)–Ru(4)–Ru(2)	106.6(1)	Ag(2)–Ru(4)–Ru(3)	58.4(1)
Ag(2)–Ru(4)–Ag(1)	58.7(1)	Ru(4)–Ag(1)–Ru(3)	62.1(1)
Ag(2)–Ag(1)–Ru(3)	60.8(1)	Ag(2)–Ag(1)–Ru(4)	62.6(1)
Ru(3)–Ag(2)–Ru(1)	60.0(1)	Ru(4)–Ag(2)–Ru(1)	58.5(1)
Ru(4)–Ag(2)–Ru(3)	60.3(1)	Ag(1)–Ag(2)–Ru(1)	107.3(1)
Ag(1)–Ag(2)–Ru(3)	59.4(1)	Ag(1)–Ag(2)–Ru(4)	58.7(1)
P(1)–Ag(1)–Ru(3)	150.4(2)	P(1)–Ag(1)–Ru(4)	143.0(2)
P(1)–Ag(1)–Ag(2)	136.3(2)	P(2)–Ag(2)–Ru(1)	127.9(2)
P(2)–Ag(2)–Ru(3)	148.7(2)	P(2)–Ag(2)–Ru(4)	150.9(2)
P(2)–Ag(2)–Ag(1)	124.8(2)		
Range of Ru–C–O		162(2)–179(3)	

It is of interest to compare the relative alignments of the C_6H_4Me-2 rings in **I** and phenyl moieties in **II** to assess the influence of the bulky *ortho* methyl groups. Fig. 5 shows the relative orientations of the phenyl rings of the two PPh_3 ligands in II [7]. Comparison of Figs. 4 and 5 reveals that the positions of the phenyl rings around P(2) in **II** are not at all dissimilar to those of the C_6H_4Me-2 groups around P(2) in **I**. However, the presence of the *ortho* methyl groups does cause a significant difference in the relative orientations of the C_6H_4Me-2 rings and the phenyl moieties around P(1) in clusters **I** and **II**, respectively. The positions of the phenyl groups around P(1) in **II** seem to be sterically favourable, with two of the three rings pointing away from the other PPh_3 ligand (Fig. 5). In contrast, only one of the three C_6H_4Me-2 rings on each of the two $P(C_6H_4Me\text{-}2)_3$ groups in **I** points away from the other phosphine ligand (Fig. 4). It is possible that the reason why the C_6H_4Me-2 moieties around P(1) in **I** do not adopt similar relative orientations to those of the phenyl rings in II is to avoid repulsion between one or more of the *ortho* methyl groups and some other part of the cluster. Alternatively, the C_6H_4Me-2 rings on the two

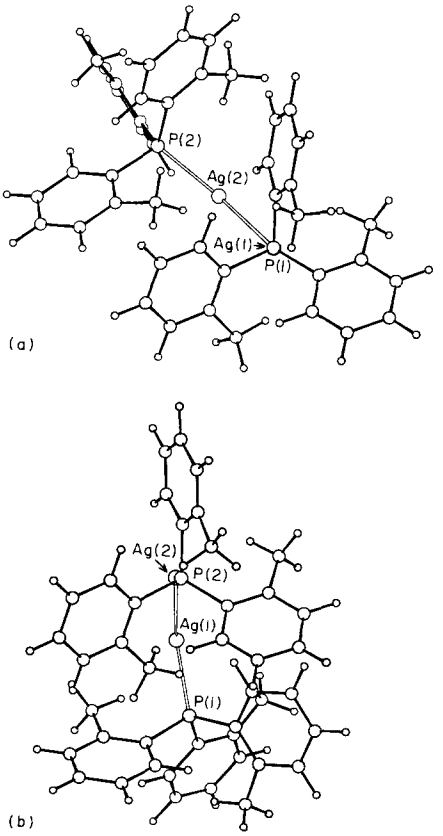

Fig. 4. Views down the Ag(1)–P(1) (a) and Ag(2)–P(2) (b) vectors of $[Ag_2Ru_4(\mu_3\text{-}H)_2(CO)_{12}\{P(C_6H_4Me\text{-}2)_3\}_2]$ (**I**), showing the relative positions of the six C_6H_4Me-2 rings on the two adjacent phosphine ligands. The ruthenium atoms, carbonyl groups, and hydrido ligands have been omitted for clarity.

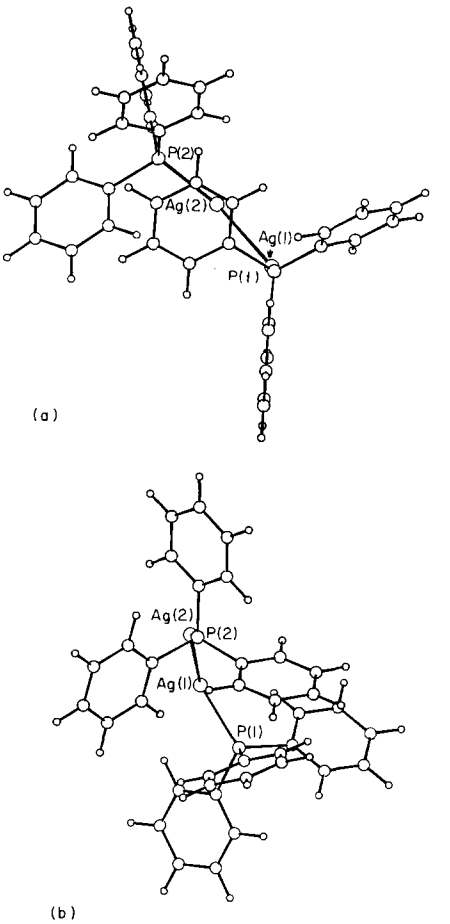

Fig. 5. Views down the Ag(1)–P(1) (a) and Ag(2)–P(2) (b) vectors of $[Ag_2Ru_4(\mu_3\text{-}H)_2(CO)_{12}(PPh_3)_2]$ (**II**), showing the relative positions of the six phenyl rings on the two adjacent phosphine ligands. The ruthenium atoms, carbonyl groups and hydrido ligands have been omitted for clarity.

$P(C_6H_4Me\text{-}2)$ ligands in **I** may not be able to interlock in a similar manner to that of the phenyl moieties in **II** because of unacceptable repulsions between an *ortho* methyl group and the C_6H_4Me-2 rings on the other phosphine in that relative alignment.

Having established the molecular structure of **I**, it is possible to interpret the variable-temperature ^1H and $^{31}P\text{-}\{^1H\}$ NMR spectra of the cluster. At ambient temperatures, the ^1H NMR spectrum of **I** consists of a complex multiplet for the aromatic protons (24 H), a singlet at δ 2.15 p.p.m. for the *ortho* methyl protons (18 H) and a broadened multiplet at ca. δ −17.1 p.p.m. for the hydrido ligand (2H). As the temperature is lowered, the signals due to the *ortho* methyl protons and hydrido ligands both broaden. At −70°C, five singlets in the ratio 3H:3H:3H:3H:6H are observed for the *ortho* methyl protons and the hydrido ligand resonance consists of two broad doublets [$J(AgP)_{av.}$ ca. 32 and ca. 24 Hz], which overlap. Unfortunately, the rather poor solubility of **I** in all common organic solvents prevented the recording of good quality ^1H NMR

spectra at temperatures below −70°C. A single phosphorus resonance, which is split into two broadened apparent doublets [$J(^{109}AgP)$ ca. 499, $J(^{107}AgP)$ ca. 432 Hz] [15] is visible in the $^{31}P-\{^1H\}$ NMR spectrum of **I** at +40°C. As the temperature is lowered, the signals broaden further and then coalesce, so that an extremely broad singlet is observed at −30°C. Again, the poor solubility of **I** hindered the measurement of good quality spectra and none could be obtained at temperatures below −40°C. Therefore, the low-temperature limiting $^{31}P-\{^1H\}$ NMR spectrum of **I** could not be recorded. However, the observation of a singlet for the *ortho* methyl protons at room temperature and a single phosphorus resonance at +40°C in the ^1H and $^{31}P-\{^1H\}$ NMR spectra, respectively, demonstrates that **I** undergoes similar dynamic behaviour, which involves an intramolecular rearrangement of the metal core, similar to that previously reported [5–7,11,12,16,17] for a number of closely related silver-containing clusters. In all of these latter species, the silver atoms exchange between the two inequivalent sites in the capped trigonal bipyramidal metal skeleton at ambient temperatures in solution, which renders the two attached phosphine ligands equivalent on the NMR timescale. The ^1H NMR spectrum of **I** at −70°C is consistent with the ground state structure of the cluster. Clearly, the intramolecular metal core rearrangement is too slow to be visible on the NMR timescale at this temperature. However, it is also interesting that the rotations around the Ag–P and $P-C_{ispo}$ bonds have been restricted [18] so that the C_6H_4Me-2 rings in the two phosphine ligands adopt conformations which remove the plane of symmetry present in the metal framework of **I** [through Ag(1), Ag(2), Ru(1), and Ru(2) in Fig. 2] and render all of the six *ortho* methyl groups inequivalent on the NMR timescale [19]. Hence, in the ^1H NMR spectrum of **I** at −70°C, a doublet is observed for each of the two inequivalent hydrido ligands and there are five signals due to the protons off the *ortho* methyl groups. Although six peaks would be expected for the latter protons, one of the observed singlets has an integration consistent with two methyl groups, so there must be an accidental degeneracy of chemical shifts in that particular case. The hydrido ligand doublets are both split by a coupling to one silver atom, as expected [5–7,11,12,16]. Additional smaller couplings to one phosphorus atom have also been previously observed [5–7,11,12,16] for the hydrido ligand signals in the ^1H NMR spectra of some silver-containing clusters, which are closely related to **I**, but the hydrido ligand peaks of **I** are still sufficiently broadened at −70°C by the dynamic behaviour of the cluster for these $^{31}P-^1H$ couplings not to be resolved. The broadening of the phosphorus signal and the hydrido ligand peaks observed in the $^{31}P-\{^1H\}$ and ^1H NMR spectra, respectively, of **I** at ambient temperatures are probably both due to a second type of dynamic behaviour. At room temperature in solution, the PPh_3 ligands in **II** [7] and the PR_3 (R = CH_2Ph [5], ^iPr [6], or Cy [6]) ligands in $[Ag_2Ru_4(\mu_3\text{-}H)_2(CO)_{12}(PR_3)_2]$ all undergo intermolecular exchange between clusters. It seems very likely that the closely related cluster **I** will also exhibit similar dynamic behaviour, and an intermolecular exchange of $P(C_6H_4Me\text{-}2)_3$ ligands is entirely consistent with the broadened signals observed in the ^1H and $^{31}P-\{^1H\}$ NMR spectra of **I** at ambient temperatures.

It is of interest to compare the work described here with some results reported by Housecroft, Rheingold, and co-workers, which demonstrate that the greater size of the $P(C_6H_4Me\text{-}2)_3$ ligand compared to the PPh_3 group can have an effect on the chemistry of Group IB metal heteronuclear clusters [20–23]. Although these workers have prepared the cluster $[Au_2Fe_4BH(CO)_{12}(PPh_3)_2]$ [20,21], they found that the $\{Fe_4B(CO)_{12}\}$ fragment was too small to accommodate more than one of the larger $Au\{P(C_6H_4Me\text{-}2)_3\}$ units and their attempts to prepare the analogous compound $[Au_2Fe_4BH(CO)_{12}\{P(C_6H_4Me\text{-}2)_3\}_2]$ failed [22]. In addition, the formal replacement of the two PPh_3 ligands in $[Au_2Ru_4BH(CO)_{12}(PPh_3)_2]$ by $P(C_6H_4Me\text{-}2)_3$ groups was found to change the skeletal geometry adopted by the cluster to one in which the greater steric requirements of $P(C_6H_4Me\text{-}2)_3$ have forced the two gold-phosphine fragments further apart on the basic $\{Ru_4B(CO)_{12}\}$ framework, with a concomitant rearrangement in the positions of the hydrido ligand and carbonyl groups [23]. At low temperatures in solution, a second skeletal isomer of $[Au_2Ru_4BH(CO)_{12}\{P(C_6H_4Me\text{-}2)_3\}_2]$ was also observed [23]. This isomer is thought to adopt a metal core structure in which the two $Au\{P(C_6H_4Me\text{-}2)_3\}$ moieties adopt positions on the basic $\{RuB(CO)_{12}\}$ framework such that there is no close contact between the gold atoms. The observation of this second skeletal isomer, which has a sterically less demanding metal core structure, for the $P(C_6H_4Me\text{-}2)_3$-containing cluster, but not for its PPh_3-containing analogue, can also be attributed to the greater cone angle of the $P(C_6H_4Me\text{-}2)_3$ ligand compared with that of the PPh_3 ligand.

3. Experimental details

The salt $[N(PPh_3)_2]_2[Ru_4(\mu\text{-}H)_2(CO)_{12}]$ was prepared as previously described [24] and the complex $[Ag(NCMe)_4]PF_6$ was made by a modification of a published route [25]. The phosphine ligand $P(C_6H_4Me\text{-}2)_3$ was purchased from Strem Chemicals, Inc., and used without further purification. The techniques used and the instrumentation employed for spectroscopic characterization have been described elsewhere [16]. Light petroleum refers to the fraction of b.p. 40–60°C.

Table 3
Fractional atomic coordinates and isotropic thermal parameters (Å^2) for $[Ag_2Ru_4(\mu_3\text{-}H)_2(CO)_{12}\{P(C_6H_4Me\text{-}2)_3\}_2]\cdot CH_2Cl_2$, with estimated standard deviations in parentheses

Atom	x	y	z	U_{iso} or U_{eq}
Ru(1)	0.19985(3)	0.05533(4)	−0.11516(6)	0.0356(3)
Ru(2)	0.08549(3)	0.11335(4)	−0.25045(5)	0.0398(3)
Ru(3)	0.24281(3)	0.25831(3)	−0.12812(4)	0.0358(3)
Ru(4)	0.11349(2)	0.19345(3)	−0.04475(4)	0.0339(2)
Ag(1)	0.22834(3)	0.39188(4)	0.03812(5)	0.0400(2)
Ag(2)	0.29963(3)	0.23726(3)	0.07137(5)	0.0361(3)
P(1)	0.24755(3)	0.56319(4)	0.13959(5)	0.0369(3)
P(2)	0.41864(3)	0.25388(4)	0.22548(5)	0.0323(2)
C(11)	0.23061(4)	0.00183(5)	−0.21885(5)	0.0622(4)
O(11)	0.24954(5)	−0.03185(5)	−0.28252(6)	0.0994(4)
C(12)	0.09936(4)	−0.05238(4)	−0.15663(5)	0.0647(4)
O(12)	0.04530(5)	−0.12233(6)	−0.16995(6)	0.0855(5)
C(13)	0.28205(4)	0.01440(5)	−0.01676(6)	0.0535(4)
O(13)	0.31260(4)	−0.03175(5)	0.02414(5)	0.0748(5)
C(21)	−0.01859(4)	0.01809(5)	−0.28537(6)	0.0864(4)
O(21)	−0.08502(5)	−0.04030(6)	−0.31249(6)	0.0820(4)
C(22)	0.03211(4)	0.19351(4)	−0.31140(5)	0.0892(4)
O(22)	0.00181(5)	0.24368(5)	−0.34886(6)	0.0850(4)
C(23)	0.09622(4)	0.05166(4)	−0.36310(5)	0.0548(4)
O(23)	0.10049(5)	0.00975(5)	−0.44212(6)	0.0875(5)
C(31)	0.25652(4)	0.20836(5)	−0.24087(5)	0.0760(5)
O(31)	0.26627(5)	0.19927(5)	−0.31922(6)	0.0856(4)
C(32)	0.35723(4)	0.34764(5)	−0.05354(5)	0.0454(4)
O(32)	0.42275(5)	0.39537(5)	−0.02877(6)	0.0667(5)
C(33)	0.20083(5)	0.35148(5)	−0.16474(6)	0.0946(4)
O(33)	0.16831(5)	0.40353(5)	−0.19768(6)	0.0810(5)
C(41)	0.05115(4)	0.27098(5)	−0.10060(5)	0.0554(4)
O(41)	0.00480(4)	0.31216(5)	−0.13365(6)	0.0745(4)
C(42)	0.00862(4)	0.09695(5)	−0.06969(5)	0.0450(4)
O(42)	−0.05019(4)	0.04152(5)	−0.07874(5)	0.0693(4)
C(43)	0.13175(4)	0.24510(5)	0.09170(5)	0.0619(4)
O(43)	0.13064(5)	0.27155(5)	0.17423(6)	0.0794(4)
C(111)	0.21087(5)	0.56077(5)	0.24034(6)	0.0388(5)
C(112)	0.23810(5)	0.50804(5)	0.30489(6)	0.0478(5)
C(113)	0.20355(5)	0.50037(5)	0.37800(6)	0.0614(6)
C(114)	0.14181(5)	0.54539(5)	0.38655(6)	0.0818(5)
C(115)	0.11457(5)	0.59814(5)	0.32204(6)	0.0717(5)
C(116)	0.14911(5)	0.60583(5)	0.24892(6)	0.0528(5)
C(117)	0.30701(5)	0.46376(5)	0.30724(6)	0.0594(5)
C(121)	0.18426(5)	0.62248(5)	0.06337(6)	0.0368(5)
C(122)	0.19664(5)	0.72345(5)	0.08435(6)	0.0527(6)
C(123)	0.14167(5)	0.75741(5)	0.01883(6)	0.0560(5)
C(124)	0.07438(5)	0.69038(5)	−0.06764(6)	0.0786(6)
C(125)	0.06203(5)	0.58939(5)	−0.08861(6)	0.0824(5)
C(126)	0.11697(5)	0.55541(5)	−0.02310(6)	0.0803(5)
C(127)	0.26811(5)	0.80093(5)	0.17960(6)	0.0835(5)
C(131)	0.35732(5)	0.64605(5)	0.19685(6)	0.0365(5)
C(132)	0.40299(5)	0.66442(5)	0.13625(6)	0.0578(5)
C(133)	0.48633(5)	0.72867(5)	0.18029(6)	0.0571(6)
C(134)	0.52402(5)	0.77456(5)	0.28497(6)	0.0694(5)
C(135)	0.47835(5)	0.75618(5)	0.34558(6)	0.0703(6)
C(136)	0.39500(5)	0.69195(5)	0.30154(6)	0.0463(5)
C(137)	0.36764(5)	0.61797(5)	0.02694(6)	0.0739(5)
C(211)	0.46091(5)	0.15307(5)	0.21115(6)	0.0345(5)
C(212)	0.49998(5)	0.13396(5)	0.14184(6)	0.0436(6)
C(213)	0.53418(5)	0.05597(5)	0.13381(6)	0.0536(5)
C(214)	0.52928(5)	−0.00290(5)	0.19511(6)	0.0768(5)
C(215)	0.49017(5)	0.01623(5)	0.26446(6)	0.0544(5)
C(216)	0.45598(5)	0.09422(5)	0.27246(6)	0.0383(5)
C(217)	0.50074(5)	0.18784(5)	0.07059(6)	0.0568(5)
C(221)	0.39087(5)	0.26676(5)	0.33588(5)	0.0323(5)
C(222)	0.31616(5)	0.20210(5)	0.32971(5)	0.0545(6)
C(223)	0.29021(5)	0.21735(5)	0.41162(5)	0.0404(5)
C(224)	0.33901(5)	0.29720(5)	0.49965(5)	0.0629(5)
C(225)	0.41376(5)	0.36185(5)	0.50579(5)	0.0373(6)
C(226)	0.43968(5)	0.34663(5)	0.42390(5)	0.0428(5)
C(227)	0.25874(5)	0.11400(5)	0.23043(6)	0.0529(5)
C(231)	0.50807(5)	0.36191(5)	0.26027(6)	0.0324(5)
C(232)	0.59189(5)	0.37347(5)	0.31992(6)	0.0520(6)
C(233)	0.65833(5)	0.45332(5)	0.33065(6)	0.0662(5)
C(234)	0.64097(5)	0.52161(5)	0.28178(6)	0.0602(6)
C(235)	0.55715(5)	0.51007(5)	0.22215(6)	0.0555(5)
C(236)	0.49071(5)	0.43018(5)	0.21141(6)	0.0419(5)
C(237)	0.61957(5)	0.31108(6)	0.38624(6)	0.0555(5)
C(1)	0.73854(22)	0.04520(26)	0.54725(28)	0.0951(14)
Cl(1)	0.63274(18)	0.01546(19)	0.53953(18)	0.0979(10)
Cl(2)	0.76262(19)	0.15909(17)	0.54352(18)	0.0891(10)

3.1. Synthesis of the cluster compound $[Ag_2Ru_4(\mu_3\text{-}H)_2(CO)_{12}\{P(C_6H_4Me\text{-}2)_3\}_2]$ (I)

A dichloromethane (40 cm^3) solution of $[N(PPh_3)_2]_2[Ru_4(\mu\text{-}H)_2(CO)_{12}]$ (0.60 g, 0.33 mmol) at −30°C was treated with a solution of $[Ag(NCMe)_4]PF_6$ (0.28 g, 0.67 mmol) in dichloromethane (30 cm^3). The mixture was stirred at −30°C for ca. 1 min and a dichloromethane (20 cm^3) solution of $P(C_6H_4Me\text{-}2)_3$ (0.21 g, 0.69 mmol) was then added. The mixture was allowed to warm to room temperature and the solvent was removed under reduced pressure. The crude residue was extracted with a dichloromethane/diethyl ether mixture (1:4 proportions; 25 cm^3 portions) until the extracts were no longer red, and the combined extracts were then filtered through a Celite pad (ca. 1 × 3 cm). After removal of the solvent under reduced pressure, the residue was dissolved in dichloromethane/light petroleum mixture (3:1) and chromatographed at −20°C on a Florisil column (20 × 3 cm). Elution with a dichloromethane/light petroleum mixture (3:1) afforded one dark red band, which, after removal of the solvent under reduced pressure and crystallization of the residue from a dichloromethane/light petroleum mixture yielded red microcrystals of $[Ag_2Ru_4(\mu_3\text{-}H)_2(CO)_{12}\{P(C_6H_4Me\text{-}2)_3\}_2]$ (I) (0.36 g, 70%), m.p. 149–152°C (decomp.). Found (for a sample of I crystallized from a diethyl ether/light petroleum mixture to avoid any dichloromethane of crystallization): C, 41.3; H, 3.0%, $C_{54}H_{44}O_{12}Ag_2Ru_4P_2$ requires: C, 41.4; H, 2.8%.

ν_{max} (CO) at 2069 s, 2031 vs, 2019 vs, 2003 s, 1985(sh), 1972 m, 1941 w(br) cm^{-1} (CH_2Cl_2). NMR: ^{1}H (CD_2Cl_2) at +25°C, ca. δ −17.1 (m vbr, 2 H, μ_3-H), 2.15 (s, 18 H, C_6H_4*Me*-2), and 7.00–7.36 (m, 24 H, C_6*H*$_4$Me-2); at −70°C, ca. δ −17.4 [d br, 1 H, μ_3-H, $J(AgH)_{av.}$ ca. 32 Hz], ca. −17.2 [d br, 1 H, μ_3-H,

$J(AgH)_{av.}$ ca. 24 Hz], 1.53 (s, 6 H, C_6H_4Me-2), 2.19, 2.24, 2.72, 2.78 (all s, 3 H, C_6H_4Me-2), and 7.12–7.68 (m, 24 H, C_6H_4Me-2); $^{31}P-\{^1H\}$ (CD_2Cl_2/CH_2Cl_2) [rel. to 85% H_3PO_4 (ext.)] at +40°C, ca. δ 5.5 ppm [apparent 2 × d br, $J(^{109}AgP)$ ca. 499, $J(^{107}AgP)$ ca. 432 Hz] [15].

3.2. Crystal structure determination for $\mathbf{I} \cdot CH_2Cl_2$

Suitable crystals of **I** were grown from a dichloromethane/diethyl ether/light petroleum mixture by slow layer diffusion at −20°C.

Crystal data for $\mathbf{I} \cdot (CH_2Cl_2)$: $C_{54}H_{44}O_{12}P_2Ag_2Ru_4 \cdot (CH_2Cl_2)$, $M = 1652.02$, triclinic, space group $P\bar{1}$ (no. 2), $a = 17.331(3)$, $b = 14.678(3)$, $c = 14.680(3)$ Å, $\alpha = 103.64(2)$, $\beta = 107.94(2)$, $\gamma = 102.40(2)°$, $U = 3281.58$ Å^3, $Z = 2$, $D_c = 1.672$ g cm^{-3}, $F(000) = 1612$. A red crystal of size 0.14 × 0.16 × 0.24 mm, μ(Mo Kα) 1.54 mm^{-1}, was used for data collection.

Data collection. Data were collected in the θ-range 3–25°, with a scan width of 0.80°, by the procedure described previously [26]. Equivalent reflections were merged to give 4354 data with $I/\sigma(I) > 3.0$. Absorption corrections were applied to the data after initial refinement of the isotropic thermal parameters of all the non-hydrogen atoms [27].

Structure solution and refinement [28]. The positions of all the metal atoms in the structure of **I** were deduced from a Patterson synthesis and the remaining non-hydrogen atoms were located from subsequent difference-Fourier syntheses. Although the two hydrido ligands were not located directly from the data, suitable positions were obtained from potential energy minimization calculations [29]. These atoms were included in the structure factor calculations, with fixed thermal parameters of 0.08 Å^2, but their parameters were not refined. The substituted phenyl rings of the ligand, $P(C_6H_4Me\text{-}2)_3$, were treated as rigid hexagons [d(C–C) = 1.395 Å] and all of the hydrogen atoms associated with each of these groups were included in geometrically idealized positions and constrained to 'ride' on the relevant carbon atoms with common group isotropic thermal parameters of 0.08 Å^2, which were not refined. The dichloromethane molecule showed signs of disorder which was not readily resolved by assigning pairs of separate sites for the chlorine atoms. The marked disorder was modelled using anisotropic displacement parameters. Anisotropic thermal parameters were assigned to the metal and the phosphorus atoms during the final cycles of full-matrix refinement which converged at R and R' values of 0.0540 and 0.0543, respectively, with weights of $w = 1/\sigma^2(F_o)$ assigned to individual reflections. The final atomic coordinates and equivalent isotropic thermal parameters for **I** are given in Table 3. Complete lists of bond lengths and angles and tables of thermal parameters and hydrogen atom coordinates have been deposited at the Cambridge Crystallographic Data Centre.

Acknowledgements

We thank Ms Carolyn J. Brown for performing some preliminary experiments, the SERC for a studentship (to P.J.M.), and Johnson Matthey plc for a generous loan of silver and ruthenium salts.

References and notes

[1] Part XVI, S.S.D. Brown, I.D. Salter and T. Adatia, *J. Chem. Soc., Dalton Trans.*, (1993) 559.
[2] I.D. Salter, in G. Wilkinson, F.G.A. Stone, and E.W. Abel (eds.), *Comprehensive Organometallic Chemistry II*, Vol. 10 Pergamon, Oxford, in press.
[3] D.M.P. Mingos and M.J. Watson, *Adv. Inorg. Chem.*, *39* (1992) 327.
[4] I.D. Salter, *Adv. Organomet. Chem.*, *29* (1989) 249.
[5] C.J. Brown, P.J. McCarthy, I.D. Salter, K.P. Armstrong, M. McPartlin and H.D. Powell, *J. Organomet. Chem.*, *394* (1990) 711.
[6] C.J. Brown, P.J. McCarthy and I.D. Salter, *J. Chem. Soc., Dalton Trans.*, (1990) 3583.
[7] M.J. Freeman, A.G. Orpen and I.D. Salter, *J. Chem. Soc., Dalton Trans.*, (1987) 379.
[8] P.J. McCarthy, I.D. Salter and V. Šik, *J. Organomet. Chem.*, *344* (1988) 411.
[9] S.S.D Brown, I.D. Salter and B.M. Smith, *J. Chem. Soc., Chem. Commun.*, (1985) 1439.
[10] C.A. Tolman, *Chem. Rev.*, *77* (1977) 313.
[11] S.S.D. Brown, I.D. Salter and L. Toupet, *J. Chem. Soc., Dalton Trans.*, (1988) 757.
[12] S.S.D. Brown, I.D. Salter, V. Šik, I.J. Colquhoun, W. McFarlane, P.A. Bates, M.B. Hursthouse and M. Murray, *J. Chem. Soc., Dalton Trans.*, (1988) 2177.
[13] T. Adatia, P.J. McCarthy, M. McPartlin, M. Rizza and I.D. Salter, *J. Chem. Soc., Chem. Commun.*, (1988) 1106.
[14] S.S.D. Brown, I.D. Salter, A.J. Dent, G.F.M. Kitchen, A.G. Orpen, P.A. Bates and M.B. Hursthouse, *J. Chem. Soc., Dalton Trans.*, (1989) 1227.
[15] Previous studies on closely related silver-containing clusters [12] suggest that the $^{31}P-\{^1H\}$ NMR spectrum of **I** at +40°C should consist of a complex multiplet. The multiplets observed for this type of cluster are due to the superimposed subspectra of the $^{107}Ag^{107}Ag$, $^{107}Ag^{109}Ag$, and $^{109}Ag^{109}Ag$ isotopomers. These subspectra are themselves further complicated by second order effects, by $^{107}Ag-^{31}P$ and $^{109}Ag-^{31}P$ couplings through one and two bonds, and by $^{107}Ag^{107}Ag$, $^{107}Ag^{109}Ag$, and $^{109}Ag^{109}Ag$ couplings [12]. However, the energy barriers for the intramolecular metal core rearrangement and the intermolecular phosphine ligand exchange processes that **I** undergoes in solution are such that the linewidth never becomes narrow enough to allow the fine structure of the phosphorus resonance of **I** to be visible at any temperature in the fast exchange regime for the skeletal rearrangement. Thus, only the values of $^1J(^{109}AgP)$ and $^1J(^{107}AgP)$ can be estimated from the $^{31}P-\{^1H\}$ NMR spectrum of **I** at +40°C.
[16] S.S.D. Brown, P.J. McCarthy, I.D. Salter, P.A. Bates, M.B. Hursthouse, I.J. Colquhoun, W. McFarlane and M. Murray, *J. Chem. Soc., Dalton Trans.*, (1988) 2787.

[17] C.P. Blaxill, S.S.D. Brown, J.C. Frankland, I.D. Salter and V. Šik, *J. Chem. Soc., Dalton Trans.*, (1989) 2039.
[18] The relatively high energy barriers observed for the rotations about the Ag–P and P–C_{ipso} bonds in **I** are presumably a manifestation of the steric interference occurring between the two bulky phosphine ligands, which are attached to adjacent silver atoms.
[19] Obviously, the relative positions of the six C_6H_4Me-2 rings in the two phosphine ligands are not necessarily the same in the solid-state structure of **I** as they are in solution at low temperatures. However, Fig. 4 does illustrate one way in which the plane of symmetry through the metal core of **I** can be removed and all of the six *ortho* methyl groups can be rendered inequivalent.
[20] C.E. Housecroft and A.L. Rheingold, *Organometallics*, *6* (1987) 1332.
[21] C.E. Housecroft, M.S. Shongwe, A.L. Rheingold and P. Zanello, *J. Organomet. Chem.*, *408* (1991) 7.
[22] C.E. Housecroft, A.L. Rheingold and M.S. Shongwe, *Organometallics*, *8* (1989) 2651.
[23] S.M. Draper, C.E. Housecroft, J.E. Rees, M.S. Shongwe, B.S. Haggerty, and A.L. Rheingold, *Organometallics*, *11* (1992) 2356.
[24] S.S.D. Brown and I.D. Salter, *Organomet. Synth.*, *4* (1988) 241.
[25] G.J. Kubas, Inorg. Synth., 19 (1979) 90; S.S.D. Brown and I.D. Salter, *Organomet. Synth.*, *3* (1986) 315.
[26] M.K. Cooper, P.J. Guerney and M. McPartlin, *J. Chem. Soc., Dalton Trans.*, (1982) 757.
[27] N. Walker and D. Stuart, *Acta Crystallogr., Sect. A*, *39* (1983) 158.
[28] G.M. Sheldrick, *SHELX 76 Program for Crystal Structure Determination*, University of Cambridge, 1976.
[29] A.G. Orpen, *J. Chem. Soc., Dalton Trans.*, (1980) 2509.